APPLICATIONS OF THERMAL NEUTRON SCATTERING IN BIOLOGY, BIOCHEMISTRY AND BIOPHYSICS.

D. L. Worcester*
Materials Physics Division
A.E.R.E., Harwell,
Oxfordshire, U.K.

Biological applications of thermal neutron scattering have increased rapidly in recent years. A bibliography for this new field of research, prepared in July, 1976 already contained seventy-five research papers (1). Although the earliest of these papers appeared as much as ten years ago, nearly all of the work has been done in the last five years. The first International conference in this field was held at Brookhaven National Laboratory in 1975 (2). The high flux reactors at Brookhaven and Grenoble have made the major contributions to developing biological applications, but the contributions of medium flux reactors have also been substantial and can be expected to increase in the next few years. Topics of biological research with thermal neutron scattering which have proved possible with medium flux reactors will be described here.

* Present address: Physics Department, Queen Elizabeth College, Campden Hill Road, London, W8 7AH.

The following categories of biological research with thermal neutron scattering are presently identified:

I) Crystallography of biological molecules by neutron diffraction. Detailed studies have been made of both small molecules and of macromolecules such as proteins.

II) Neutron small-angle scattering of biological molecules in solution. These studies have already included numerous measurements of proteins, lipoproteins, viruses, ribosomal subunits and chromatin subunit particles.

III) Neutron small-angle diffraction from fibrous biological materials. Studies have been made of collagen, muscle, chromatin and celluloses.

IV) Neutron small-angle diffraction and scattering from biological membranes and membrane components. Studies have been made of multilamellar samples and of dispersions.

(V) Neutron quasielastic and inelastic scattering studies of the dynamical properties of biological molecules and materials.

This paper will be concerned almost exclusively with low resolution structural studies; i.e. categories II-IV.

The basic motivation for structural studies in biology with neutrons is the large difference in the coherent scattering amplitude of hydrogen (-0.374×10^{-12} cm) and deuterium (0.667×10^{-12} cm). This difference is large compared to the coherent scattering amplitudes of other atoms found in biological materials (Table 1) and therefore hydrogen-deuterium exchange provides a means of locating individual hydrogen atoms or hydrogenous molecular groups, even from rather limited

diffraction data, and evaluating the relative locations of regions of different scattering densities. Most biological materials are studied in an aqueous environment, whose scattering density can be varied over a wide range with H_2O/D_2O mixtures. This "contrast variation" procedure is particularly useful for structural analysis of biological materials with regions of different scattering densities because the neutron scattering densities of biological materials fall between that of H_2O and of D_2O (Table 1).

TABLE I

Neutron Coherent Scattering Amplitudes and Densities

nucleus	amplitude	molecular group	scattering amplitude density
H	-0.374×10^{-12} cm	H_2O	-0.0056×10^{-12} cm/A^3
D	0.667	D_2O	0.064
C	0.665	Protein	0.015-0.023
N	0.940	DNA	0.034
O	0.580	RNA	0.035
P	0.517	$(CH_2)_n$ (liquid)	-0.0034
S	0.285	Lecithin polar group	0.018

Variations of scattering densities in biological materials are of two kinds: intermolecular and intramolecular. Except for detailed crystallographic analyses, the structural information is only of rather low resolution so that the scattering densities are not those of individual atoms, but of regions occupied by many atoms. These scattering densities are defined as the sum of the scattering amplitudes of the atoms in the particular region, divided by the volume of the region. For whole molecules, the sum is over all the atoms of the molecule, and the volume is the partial specific volume of the molecule. The neutron scattering densities of proteins, nucleic acids and lipids are sufficiently different that structures containing two or more of

these components give very different scattering patterns in different H_2O/D_2O mixtures. For lipids, there is substantial variation of scattering density within the molecules: the polar groups being much higher scattering density than the hydrocarbon regions. This low-resolution intramolecular variation of scattering density also occurs in proteins, and is primarily the consequence of the wide variation of peptide scattering densities which constitute the protein (Figure 1). Polar peptides (or amino acid residues) generally have higher scattering densities than apolar peptides, but there are a few exceptions, such as lysine, which is polar but of low scattering density. Scattering

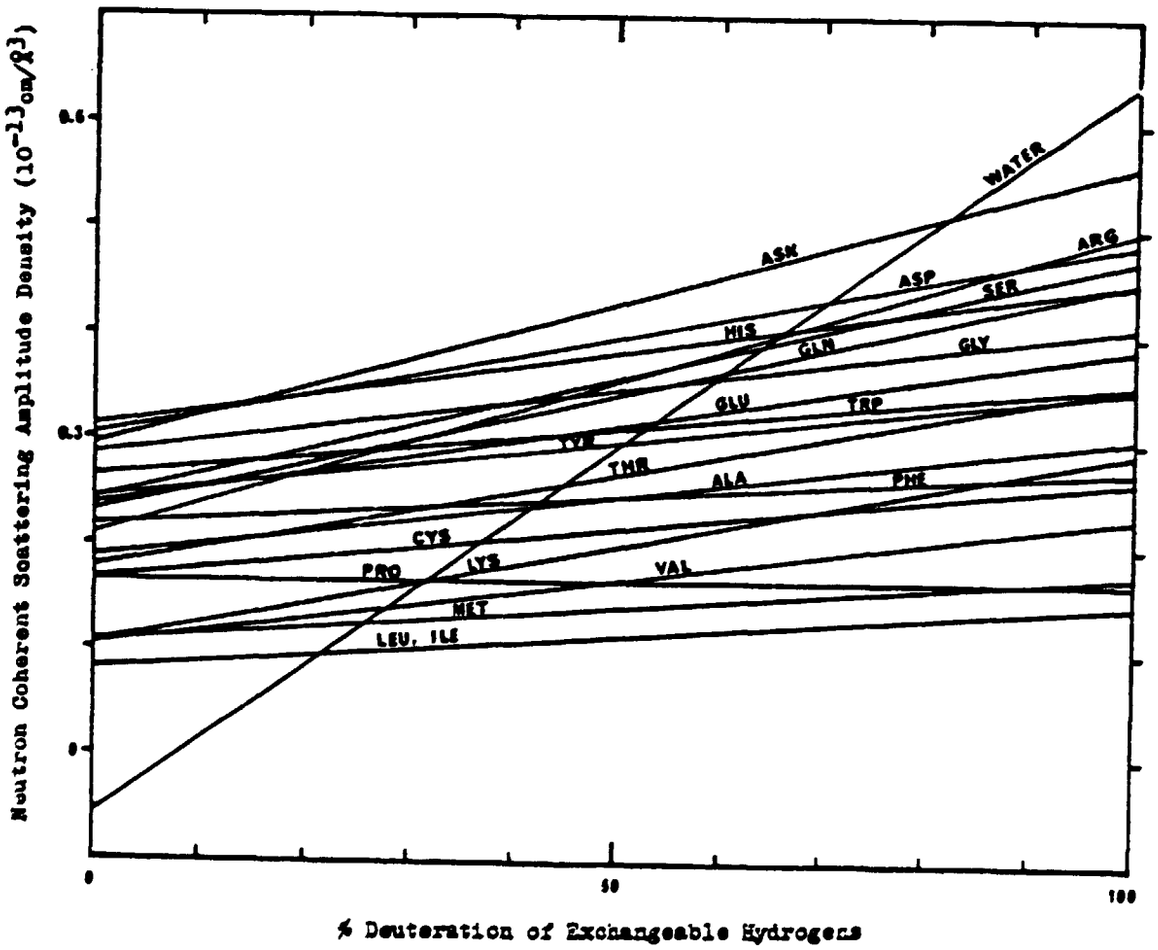

Fig. 1) Neutron scattering amplitude densities of amino acid residues.

densities of proteins are largely determined by the peptide composition, so that different proteins have different scattering densities, but are in the range of the scattering densities of 35–50% D_2O (Figure 2). The high scattering densities of collagen and silk fibroin are a consequence of the high glycine contents of these proteins, whereas the lower scattering density of histone F1 is largely a consequence of its high lysine content. Most proteins have mean scattering densities close to that of 40% D_2O. Intramolecular variation of protein scattering density usually results from having polar, hydrophilic regions as well as apolar hydrophobic regions in a protein. Thus the hydrophobic cores of the proteins elastase and subtilisin have considerably lower scattering densities than the full molecules (Figure 2).

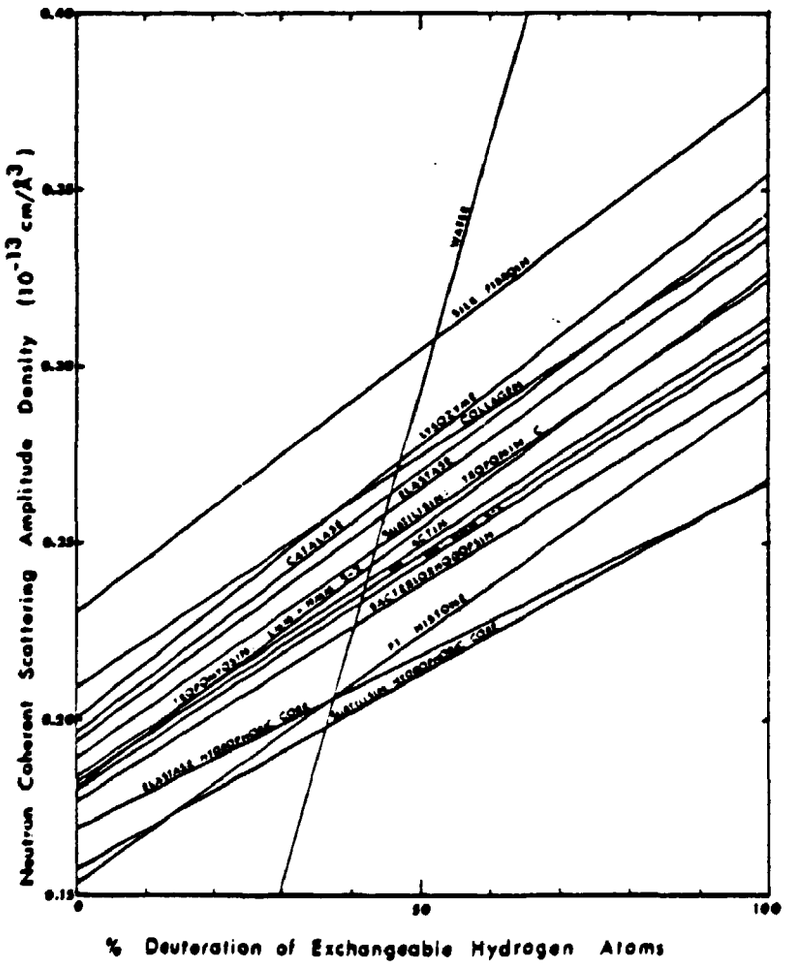

Fig. 2) Neutron scattering amplitude densities of proteins calculated from the amino acid compositions. Hb=hemoglobin, Mb=myoglobin, HMM=heavy meromyosin, LMM=light meromyosin.

These types of scattering density variations in biological materials make neutron scattering studies particularly worthwhile for low-resolution structural analysis. Some specific examples will be presented here, with emphasis on studies made at the medium flux reactor PLUTO at Harwell. The instrument used for these studies is shown in Figure 3. The neutron beam emerging from the reactor is filtered by polycrystalline beryllium to remove wavelengths shorter than 3.95Å, and by single crystals of bismuth to attenuate unwanted gamma radiations and fast neutrons. The beam is then conducted away from the reactor by a guidetube of ordinary copper waveguide. This serves to maintain the neutron flux for a beam divergence given by the critical angle of reflection and therefore the diffractometer can be placed several metres from the reactor, where there is room for better shielding from background radiations. A detail of the diffractometer is shown in Figure 4. The main feature, and somewhat unconventional aspect of this design is that the monochromator is located after the sample, and the detector of large aperture is placed close to the monochromator. This permits use of monochromators (pyrolytic graphite) of different mosaic

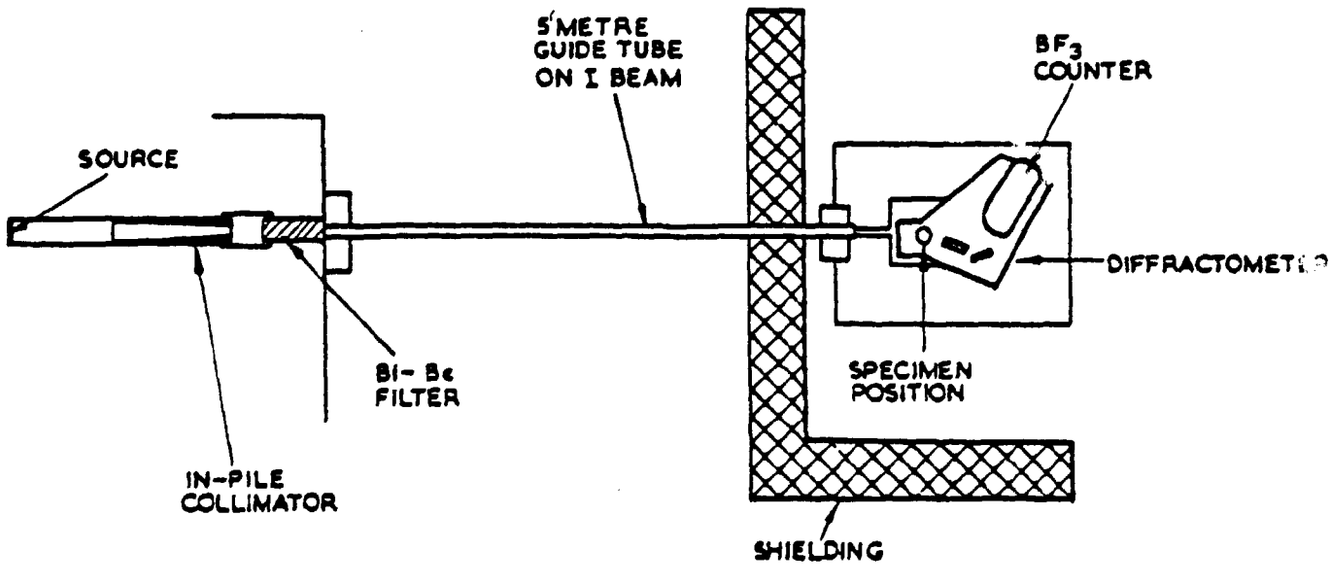

Fig. 3) Harwell guide tube and diffractometer for small-angle neutron scattering and diffraction from biological materials.

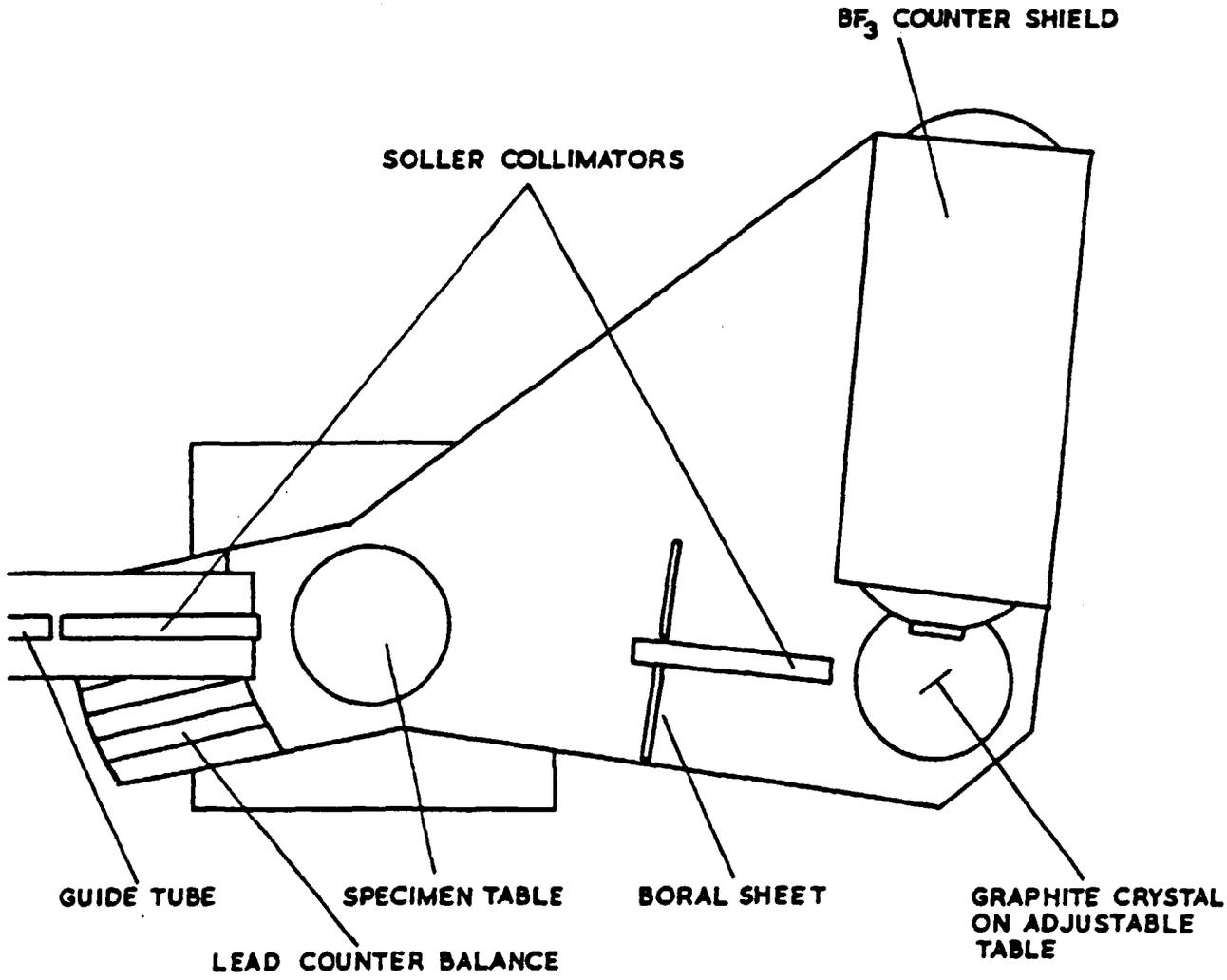

Fig. 4) Detail of diffractometer.

spreads, thereby providing the $\Delta\lambda/\lambda$ most compatible with particular experiments. For example, in radii of gyration measurements, $\Delta\lambda/\lambda$ can be quite large (e.g. 10-20%), whereas in measurements at higher angles and in measurements of diffraction peaks from fibrous or lamellar structures $\Delta\lambda/\lambda$ may need to be reduced to 1% or less. With the monochromator after the sample, nearly full use of the neutron flux within $\Delta\lambda/\lambda$ is made; and is unaffected by the collimation conditions. More detailed information on this instrument is given in ref. 3. A similar instrument was originally used at Brookhaven for biological studies (4,5).

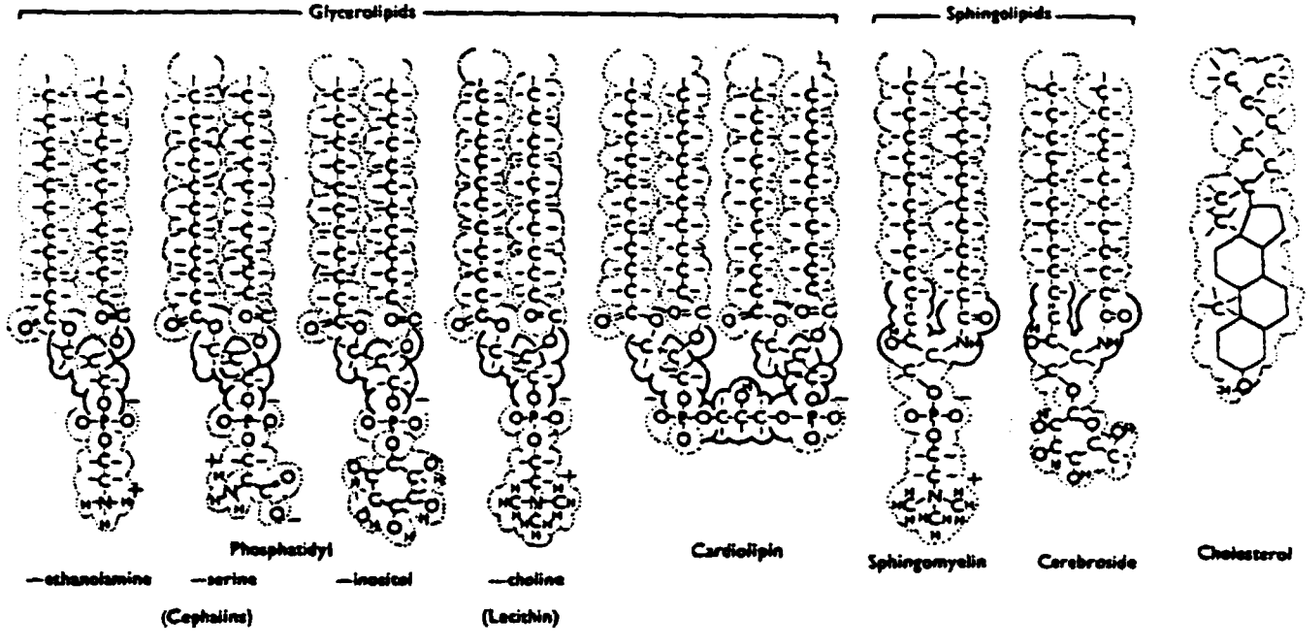

Fig. 5) The chemical formula of the major lipids of membranes drawn to illustrate their approximate spatial appearance. (From FINEAN, J. B. (1961). In *Chemical Ultrastructure in Living Tissue*. Charles C. Thomas, Illinois.)

Small-angle diffraction studies of multilayers of membrane lipids have been projects of major research with the Harwell instrument (6-8). Some of the lipids commonly found in biological membranes are shown in Figure 5. These molecules are typically of 700 to 1000 daltons molecular weight, and are amphiphilic, that is they have both a distinctly hydrophobic portion consisting of hydrocarbon, and a hydrophilic portion, often containing phosphate and/or other charged, polar groups. In an aqueous environment these lipids often spontaneously form centrosymmetric layers two molecules thick (bilayers) in which the hydrocarbon chains form a hydrophobic centre with the polar groups in contact with the water. This is only one type of many structures which these lipids form with water however and the phase behaviour, even of just the lamellar phases can be quite complex (9-11). The lamellar phases are probably the most pertinent to membrane structures, and it should be noted that in these cases the lipids are essentially smectic liquid crystals which undergo both thermotropic and lyotropic phase transitions. In the structural studies described here, the lipids were lecithins, in some cases in admixture with cholesterol. Both of these lipids are important componenta of mammalian membranes.

Fig. 6) X-ray diffraction pattern from L-α dipalmitoyl lecithin bilayers. (from J. Torbet, ref. 12).

The type of diffraction produced by a lipid sample is shown in Fig. 6 as an X-ray diffraction photograph from a specimen of dipalmitoyl lecithin (L - α dipalmitoyl phosphatidyl choline) obtained by Dr. J. Torbet (12). Several orders of lamellar diffraction are observed, as well as more diffuse diffraction at right angles, due to the packing of hydrocarbon chains. The diffraction is described as small-angle in the sense that the lamellar repeat unit, or Bragg spacing, is 50-60 Å for many of these lipids, so that the orders of diffraction are separated by only a few degrees.

Neutron diffraction from bilayers of dimyristoyl lecithin are shown in Figure 7. The diffraction data is of similar resolution to that obtained with X-rays and the time required for data collection is the same. However, rather larger amounts of sample are required for the

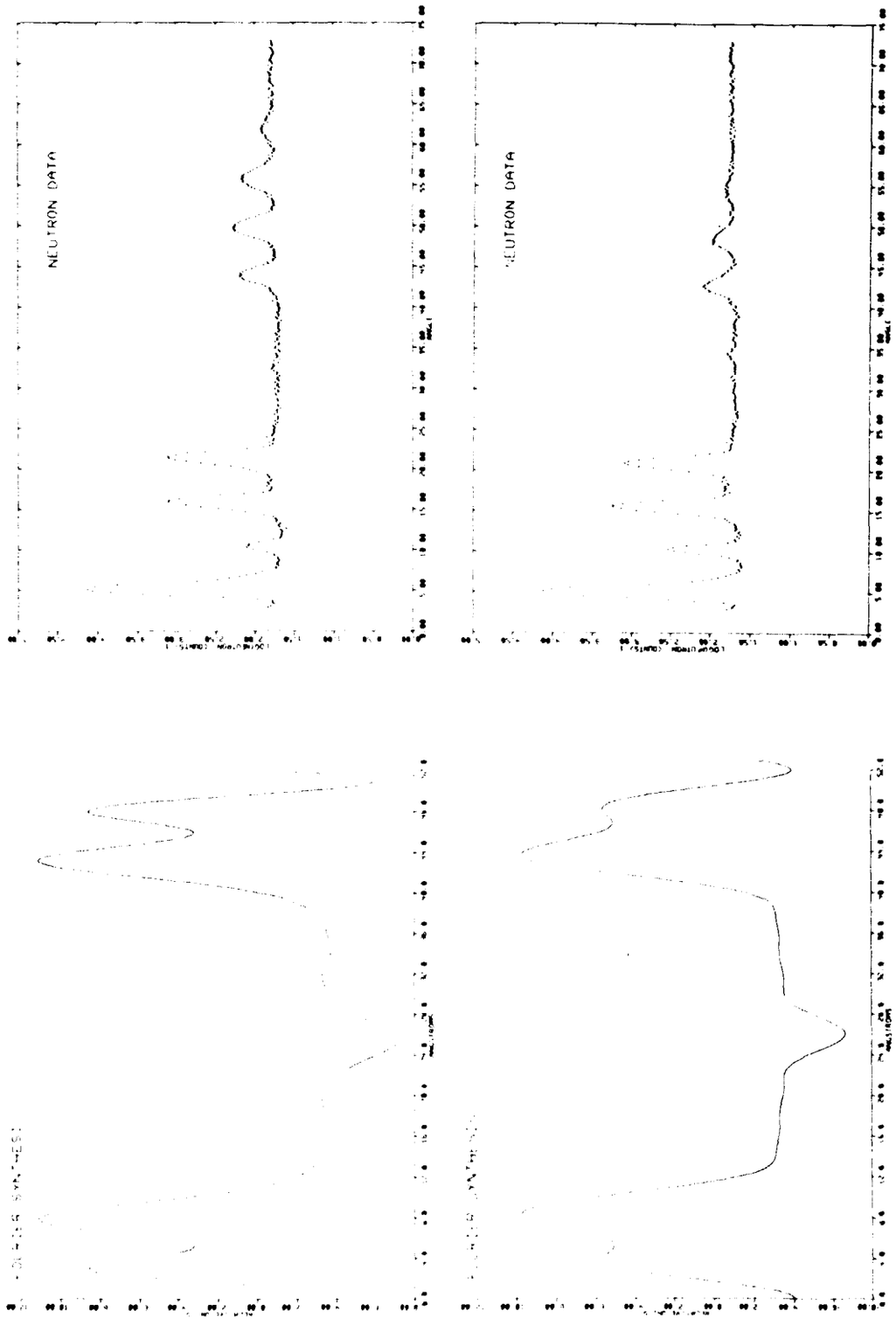

Fig. 7) Neutron diffraction data and Fourier profiles of dimyristoyl lecithin bilayers. λ =4.73Å. Top: Sample dried at 0% relative humidity, d=50.9±0.3Å. Bottom: Sample hydrated at 15% relative humidity (H_2O), d=52.0±0.3Å.

neutron studies: for the data of Figure 7, the amount is 35 mg and the measuring time 24 hrs. The main information of such diffraction data is contained in the diffraction intensities, and from these intensities the scattering density across the bilayer can be calculated. The experimental intensities must be corrected for absorption, and the diffractometer acceptance, and then the modulus of each structure factor can be calculated by applying the Lorentz factor of n to the corrected intensity: $|F_n| = (nI_n)^{\frac{1}{2}}$ where n is the order of Bragg diffraction (6-8). The scattering density across the bilayer is centrosymmetric and therefore given by

$$\rho(x) = \sum_{n=1}^{nmax} \pm |F_n| \cos 2\pi nx$$

where x is the fractional co-ordinate across the bilayer. The $\pm$ sign represents the phase problem and assignment of + or - must be made to each $|F_n|$. Several ways of emp rically establishing phase assignments are discussed in ref. 6. One of these is specific to neutron scattering and involves hydrating the sample with at least 3 different H_2O/D_2O

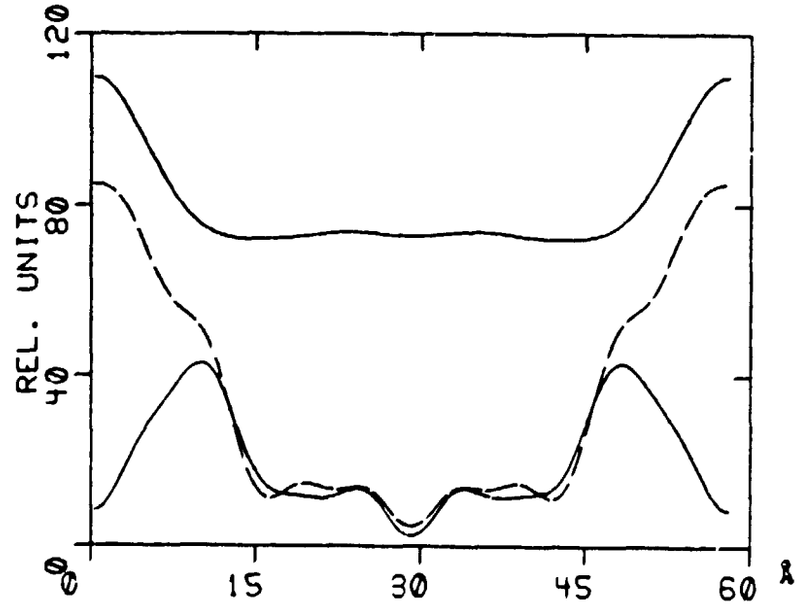

Fig. 8) Fourier profiles of neutron scattering density in L-α dipalmitoyl lecithin bilayers, hydrated at 84% relative humidity. Solid line: H_2O. Dashed line: D_2O. The upper curve is the difference profile (half-scale) for the distribution of water in the bilayer.

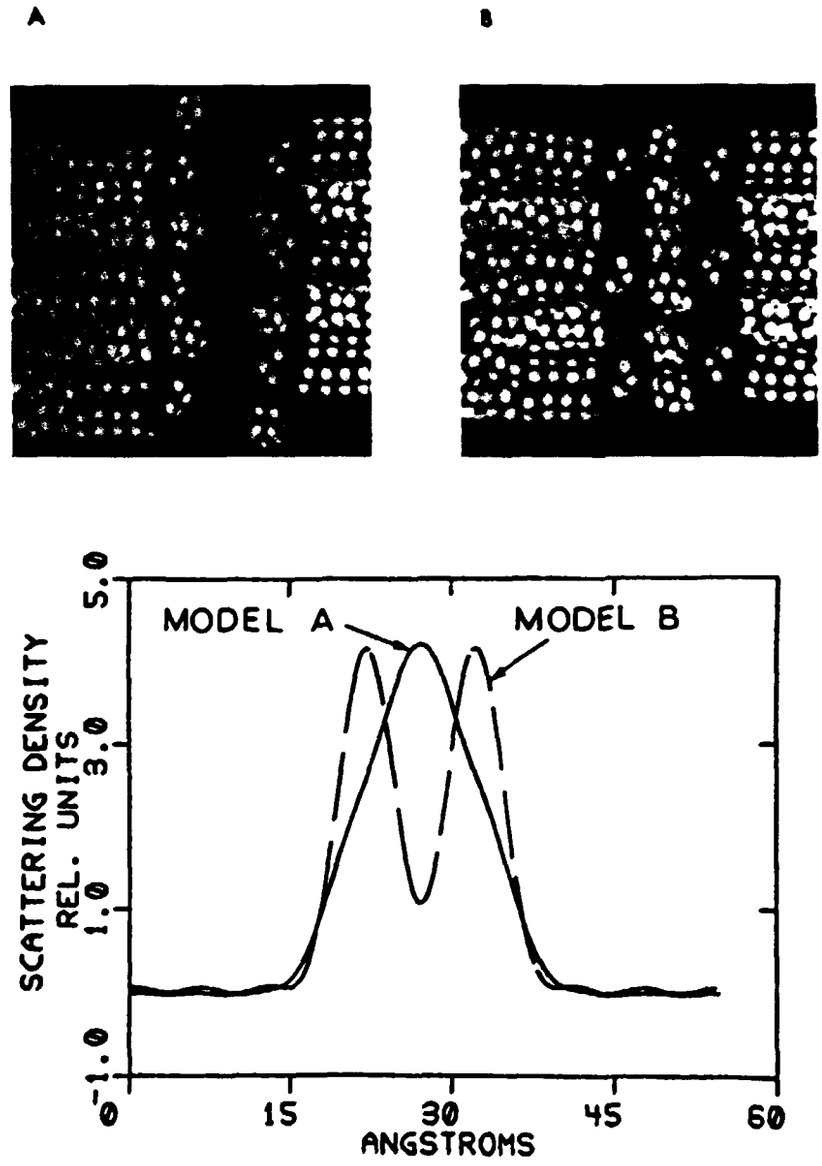

Fig. 9) Molecular models and corresponding water distributions for egg lecithin-cholesterol bilayers with two different conformations of the polar head group.

mixtures. For centrosymmetric structures, F_n is linear with the D_2O molar fraction and therefore changes of sign are established (7). If reasonable assumptions can be made about the location of water in the bilayers, then absolute phase assignments can be made. Usually this can be done reliably for the first few diffraction orders, but not for higher orders unless details of the locations of water in the bilayer are known. Fourier profiles for the dimyristoyl lecithin neutron diffraction data are shown in Figure 7. Several features of the bilayer

structure are easily identified from a knowledge of the scattering densities of the different parts. The broad,low, central scattering density is the hydrocarbon region with a central trough due tc the terminal methyl groups of the hydrocarbon chains. The high scattering density bordering the hydrocarbon region is due to the ester bonds where the fatty acid chains are connected to the glycerol molecule. The other peak in the polar group region corresponds to the phosphate group. The two profiles are slightly different in this region, and indicate that a conformational change occurs in the polar group as the hydration increases (6,7).

A particularly useful application of neutrons in structural analysis of these bilayers is in locating the water of hydration. Fourier profiles can be obtained for the bilayers hydrated with both H_2O and D_2O, and the difference profile shows only the location of the water. Such profiles, obtained from diffraction data of dipalmitoyl lecithin bilayers, are shown in Fig. 8. These water distributions can be quite useful in structural analysis. For example, different conformations of the polar groups result in different distributions of water, simply because the water cannot occupy the same space as the polar group. An example is shown in Fig. 9 in which models of egg lecithin and cholesterol bilayers are shown for two extreme conformations of the choline groups together with the corresponding water distributions. The experimentally determined distribution (8) shows only a single Gaussian-like peak, and so the structure must be the folded configuration in Fig. 9 rather than the extended one.

Another very specific application of neutrons in structural analysis of these lipid bilayers is deuterium labelling. Deuterium can often be covalently incorporated into lipid molecules by chemical means and neutron diffraction data obtained from bilayers of these lipids.

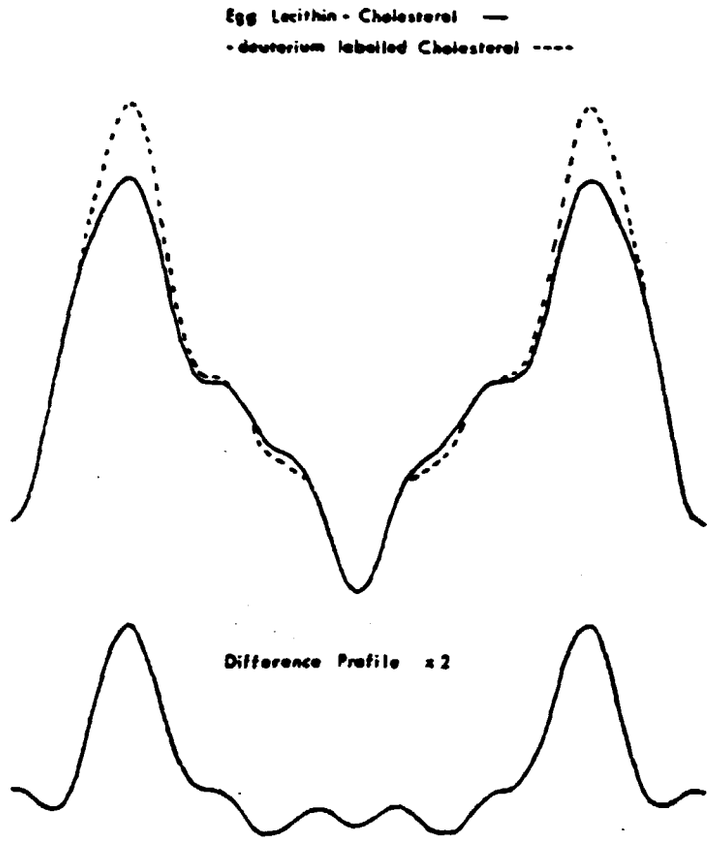

Fig. 10) Neutron scattering density profiles of bilayers of egg lecithin and A) cholesterol, B) cholesterol covalently deuterium labelled adjacent to the hydroxyl group. The difference profile (top) shows the deuterium label is 18Å from the bilayer centre The scale of profile A relative to B was established by measuring the H_2O-D_2O difference profile for both samples ("direct scaling" - see ref. 8).

Comparison is then made of profiles of the deuterium-labelled bilayers and the unlabelled bilayers. This comparison can be direct by using the water profiles of both samples as a means of scaling(6-8). When this is done, the difference between the two profiles shows the location of the deuterium label. An example is given in Figure 10 where neutron scattering density profiles of egg lecithin and cholesterol bilayers are shown. In one of the samples a single deuterium atom has been covalently bonded to the cholesterol carbon atom bearing the hydroxyl group. The difference profile shows the position of the deuterium atom, and hence that the hydroxyl group is located just at the edge of the polar hydrophilic region.

Structural studies of biological membranes are generally more difficult than for lipid bilayers. However, very limited diffraction data can often be valuable. This was found to be the case in a neutron diffraction study of the gas vesicle wall of the marine algae Anabaena flos-aquae. The gas vesicles apparently perform a valuable function by making the algal cells more bouyant and keeping them close to the marine surface where there is more light for photosynthesis. The vesicles are unusual in that they contain gas instead of water and that the vesicle wall has a very high protein content, while apparently lacking lipids and carbohydrates (13,14). It has been proposed that the inner surface of the vesicle wall is much more hydrophobic than the outer surface (15,16).

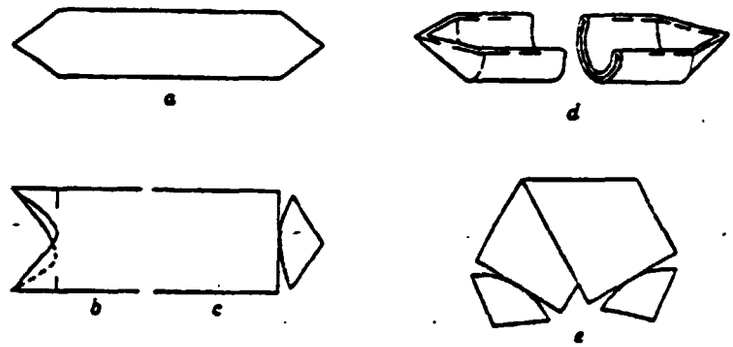

Demonstrating different ways in which gas vesicles might collapse. *a*, Intact vesicle; *b–e*, collapsed vesicles

Fig. 11) Schematic representation of intact and flattened algal gas vesicles (from A.E. Walsby, Proc. Roy. Soc. B 178, 320, 1971).

A neutron diffraction study was made to test this hypothesis. A few milligrams of collapsed vesicles (Figure 11) oriented on a glass substrate formed a specimen. In this way, the lamellar repeat unit is centrosymmetric and consists of two wall thicknesses. If the inner surface of the vesicle walls are hydrophobic and only the exterior is hydrophilic, then with D_2O hydration, the first order neutron diffraction intensity would be largest, as a consequence of the nearly sinusoidal variation of scattering density with the periodicity of the double wall. If both the inn and outer surfaces are hydrophilic then the second order diffraction intensity would be large because the sinusoidal variation of scattering density would have the periodicity of the single wall.

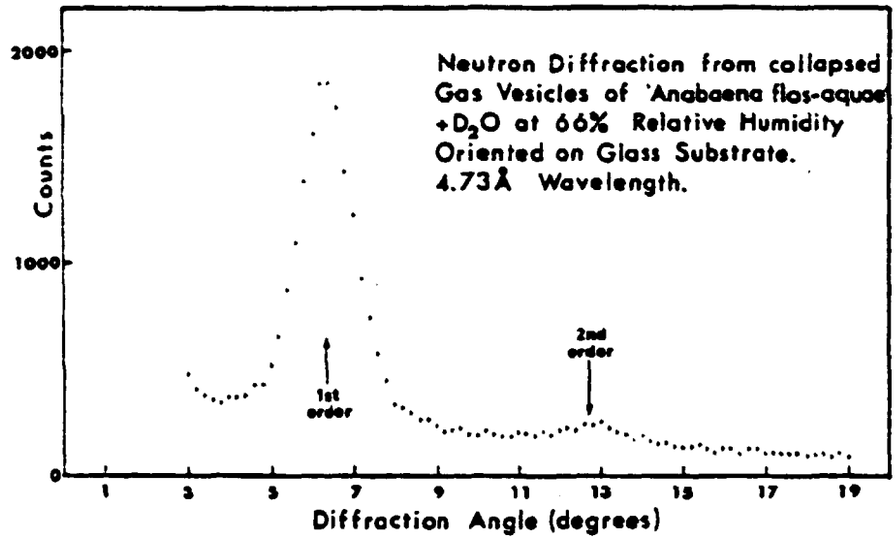

Fig. 12) Neutron diffraction data from collapsed gas vesicles of Anabaena flos-aquae hydrated with D_2O at 66% relative humidity and oriented on a glass substrate. $\lambda = 4.73\text{Å}$.

The neutron diffraction data (Figure 12) show a very strong first-order diffraction intensity relative to the second order, and therefore the inner wall must be hydrophobic. Fourier profiles obtained for several different hydrations and H_2O/D_2O mixtures, show that the inner surface of the wall has a scattering density comparable with that of H_2O, which is much lower than expected for a protein structure. This could be accounted for by the high content of leucine and isoleucine in the protein (13) if the low scattering density side chains of these and other hydrophobic peptides are located on the inner surface of the vesicle wall.

Other biological membranes that have been studied by neutron scattering are photosynthetic membranes(17). Rather little is known about the structure of these membranes, even though they perform some of the first steps in the biochemical processes of converting light energy to chemical energy. Two simple but important features of these membranes were demonstrated in a neutron small-angle scattering study made at the Institut Laue-Langevin, Grenoble using the area detector of the instrument D-11. These features are that magnesium ions are required for the pairing of the membranes at their outer surfaces and that the so-called "partition region" formed by this pairing is

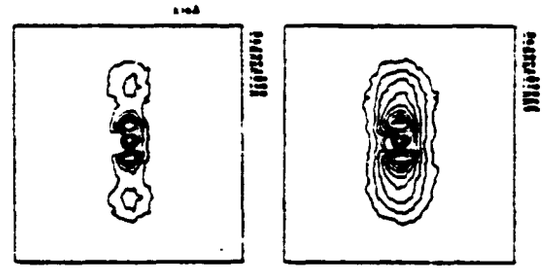

Fig. 13) Contour plots of neutron scattering data from spinach chloroplasts oriented in a magnetic field of 17 kgauss (vertical). Right: Magnesium ions present in D_2O suspending buffer. Left: Magnesium ions absent.

hydrophilic (17). The neutron scattering patterns are shown in Fig. 13 as contour maps of diffraction data collected with the two-dimensional detector. The membranes suspended in D_2O buffer were placed in a quartz cuvette between the poles of an electromagnet. In the field of 17 K gauss the membranes orient perpendicular to the magnetic field as a consequence of their diamagnetic anisotropy. The strong lamellar scattering from the membranes in D_2O buffers is therefore well oriented. When magnesium ions are present in the buffer, (left-hand side of Fig. 13) an interference maximum is observed. From the position of this interference maximum we can conclude that the membranes are paired; and from its strong intensity, we can conclude that D_2O must be present in the "partition region" between membranes (i.e. the scattering is that from a double slit rather than that from a single slit of the same total width). When magnesium ions are absent from the suspending buffer, the interference maximum is absent, and the scattering is similar to that of a single slit (right-hand side of Fig. 13).

Another important area of biological application is neutron small-angle scattering from macromolecules in solution. The first measurements of this kind were made at the medium flux reactor at Jülich (18,19), and were followed by the work of Stuhrmann at the Institut Laue-Langevin (20-27) in which a clear and useful formalism for contrast variation studies was developed and applied to a number of macromolecules in solution. The information obtainable from small angle scattering studies is primarily the size, specific volume, and molecular weight of the solute particles (28). Information on the shape of the particles can also be obtained if the scattering can be measured at larger angles than the Guinier region. In neutron scattering, contrast variation with H_2O/D_2O mixtures provides a measure

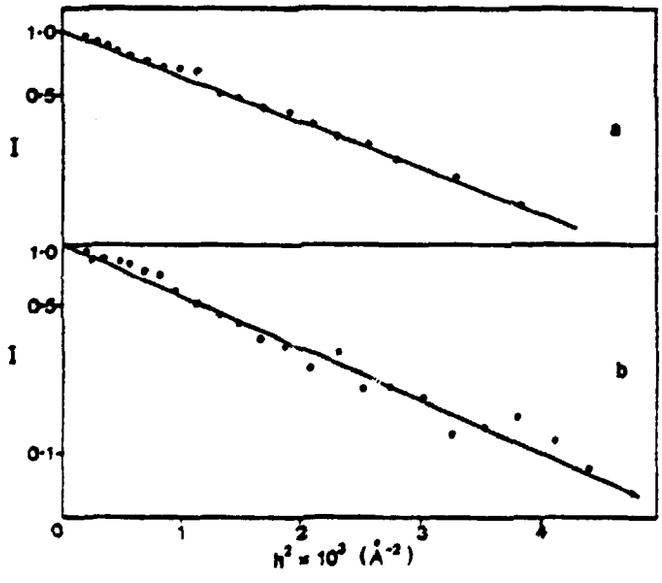

Fig. 14) Guinier plots of neutron small-angle scattering data from chromatin subunit particles (ref. 29). a) Particles in D_2O buffer. b) in H_2O buffer. $h=Q=4\pi \sin\theta/\lambda$ and 2θ is the scattering angle.

of the effective size as a function of the contrast, or difference between the scattering densities of solute and solvent. This permits direct assessment of the relative locations of the components of different scattering density.

At Harwell, neutron small-angle scattering studies of biological macromolecules in solution were made by John Pardon and co-workers of the Searle Research Laboratories (29). Their interest was in the subunit particles obtained from chromatin by nuclease digestion. These subunit particles had been characterized biochemically and were known to consist of two each of the four types of histone proteins complexed with a length of deoxyribonucleic acid (DNA) of about 140 base pairs. The original objective of the neutron scattering measurements was to determine the size of the subunits, and the relative locations of protein and nucleic acid. Measurements in the small-angle region (Guinier region), are shown in Figure 14. The radii of gyration are obtained from the slopes of these Guinier plots since in the small-angle region, the scattering has the form:

$$I(Q^2) = I_o \exp(-R_g^2 Q^2/3) \qquad \text{where } Q=4\pi\sin\theta/\lambda$$

and R_g is the radius of gyration (28). The measured radii of gyration are different for different H_2O/D_2O mixtures. This demonstrates that the low-resolution scattering density is not uniform in the subunit particles, as would occur from spatial separation of protein and nucleic acid. In the Stuhrmann formalism for contrast variation studies (21,22) the radius of gyration is given by

$$R_g^2 = R_o^2 + \alpha/\bar{\rho} - \beta/\bar{\rho}^2$$

where α and β are constants and $\bar{\rho}$ is the contrast or difference between the mean scattering density of the solute and that of the solvent. R_o is the radius of gyration at infinite contrast; that is, under conditions in which the scattering density variations within the solute

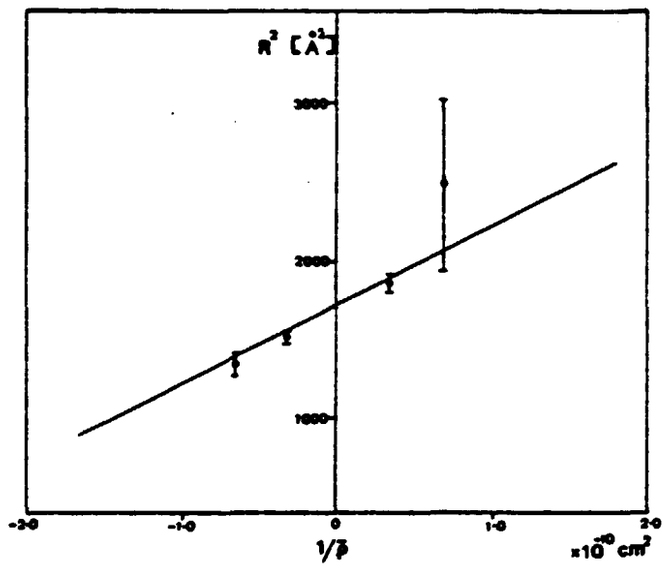

Fig. 15) Stuhrmann plot demonstrating the variation of R_g^2 as a function of $1/\bar{\rho}$ for chromatin subunit particles (ref. 29).

Table II

Radii of Gyration of Chicken Erythrocyte Chromatin Subunit Particles for Various Contrast Conditions.

	$1/\bar{\rho}$ (cm^2)	R(Å)
$R = R_p$ (protein dominates)	-1.49×10^{-10}	30.6(±2.0)
$R = R_d$ (DNA dominates)	1.69×10^{-10}	50.3(±1.4)
$R = R_o$ (infinite contrast)	0	41

particles are negligible compared to the variation between solute and solvent. R_o is therefore the radius of gyration of the volume occupied by the particle. A useful presentation of contrast variation results is in the form of a Stuhrmann plot (20,22,24,26,27) in which R_g^2 is plotted against $1/\bar{\rho}$. The data for chromatin subunit particles are shown in Figure 15. The slope of this plot gives a positive value for α, which demonstrates that the component of higher scattering density (the DNA) is toward the outside of the subunit (29). The intercept at $1/\bar{\rho} = 0$ gives R_o, the radius of gyration at infinite contrast, and is the best measure of the overall size of the subunits. The lack of curvature in the plot indicates that β is small, and therefore that the components of different scattering densities share the same centre of mass, or very nearly so. It is noted that whereas α may be positive or negative, β must be positive; a consequence of it being related to the spatial separation of centres of mass (22). Measurements at low contrasts are necessary for accurate determination of β and are often difficult at medium flux reactors. The original measurements at Harwell have been considerably improved in the work of the Portsmouth group using facilities at the Institut Laue-Langevin (30). The area detector used for these studies particularly improves data collection rates, and such instrumentation at medium flux reactors would be major assets.

From the Stuhrmann plot of Fig. 15, it is possible to estimate the radii of gyration of the protein and nucleic acid components. When the aqueous scattering density is that of the nucleic acid component (about 62% D_2O), the radius of gyration is determined predominantly by the protein, and vice-versa. The radii of gyration so obtained are given in Table II.

It is emphasized that small-angle scattering measurements of biological molecules in solutions of high contrast (H_2O, D_2O) are relatively easy to make at medium flux reactors if the radii of gyration

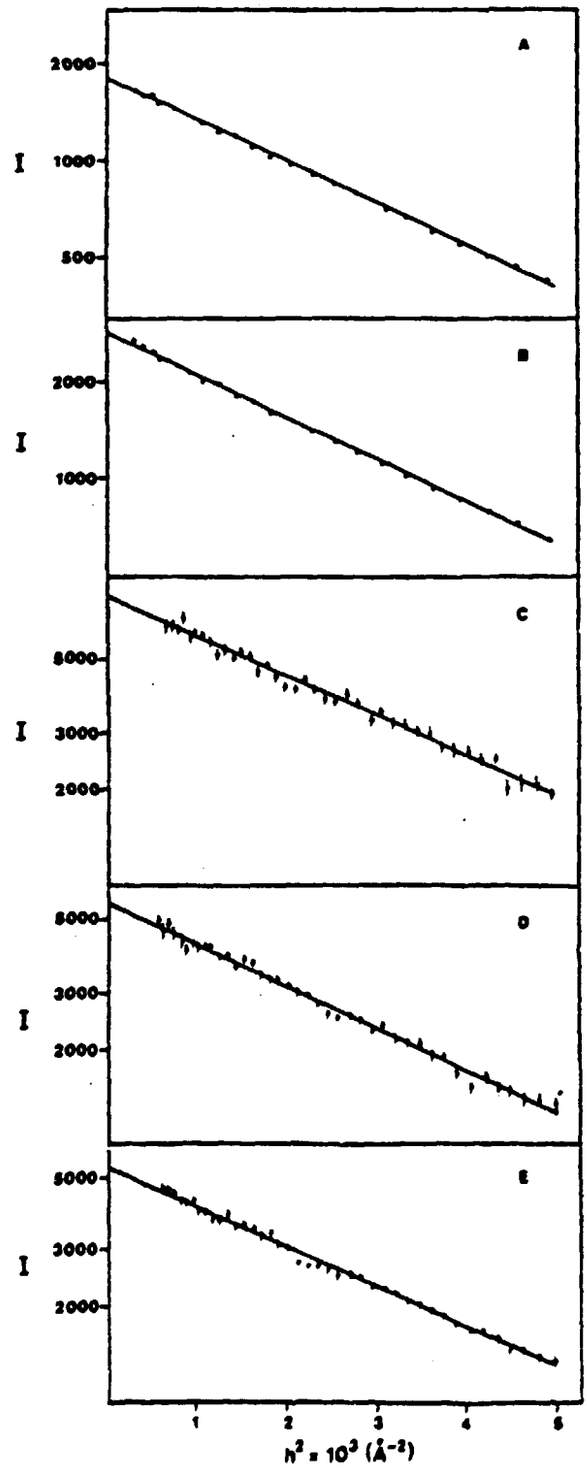

Fig. 16) Guinier plots of neutron small-angle scattering data obtained from solutions of chicken erythrocyte chromatin core protein in 2M NaCl D_2O phosphate buffer. A)2.5mg/ml B) 7mg/ml C) 10mg/ml D) 17mg/ml E) 34mg/ml.

are not larger than about 50-100 Å. This was particularly demonstrated when the Searle group extended their original studies of the chromatin subunits to include measurements of a complex of histone proteins that can be isolated from chromatin in high salt (2M NaCl). Guinier plots of small-angle scattering data obtained from solutions of these proteins are shown in Figure 16. Measurements at several different concentrations, such as shown here are important in small-angle scattering work, to ensure that the measured radius of gyration is not influenced by particle interactions. If the radius of gyration is not constant with concentration, then the values must be extrapolated to infinite dilution (28). The complex of histone proteins was found to have a constant radius of gyration of about 30 Å over the concentration range studied (2.5-35 mg/ml). This is in good agreement with the radius of gyration of the subunit particles under conditions where the protein dominates (Table II), but this agreement is not sufficient to establish that the two complexes are the same. Other important information is the molecular weight of the isolated complex, and can be determined from the zero-angle scattering intensity (I_o). Normalization of this intensity can be made by measuring the scattering from protein standards of known molecular weight (31), or by using the incoherent scattering from H_2O (27,32). The molecular weight so obtained for the histone protein complex is only half that expected for the protein of the chromatin subunits. The radii of gyration and molecular weight data can be made compatible, however, if the isolated protein complex is disc-shaped and two are stacked together in the chromatin subunits. If the height is small compared to the radius of such disks, then the radius of gyration of a stacked pair is little different from the single disk. This results from the relation $R_g^2 = R^2/2 + H^2/12$ for cylinders, where R is the radius and H is the height. For disc-shaped structures the first term, involving only the radius, dominates.

Information on the shape of particles in solution is also contained in the higher angle scattering (20-27,28). Data obtained for the chromatin subunits and the isolated complex of histone proteins are shown in Fig. 17 (33). The Guinier region, from which the radii of gyration were obtained, extends out only to about 2-3°, i.e. $QR_g \lesssim 1$. Structural analysis using also the higher angle scattering amounts to finding structures whose spherically averaged scattering is the same as that which is measured. One procedure is simply trial and error, in which the scattering from a proposed structure is calculated, usually using the Debye formula (28), and compared with the experimental scattering. Fortunately the scattering from many simple shapes have been tabulated (34-36) so that a rough shape, in terms of the axial ratios of an ellipsoid for example, can be fairly easily assessed. More complicated shapes can be problematic. A major contribution of neutron scattering is the use of contrast variation to isolate the intensity function which is due only to the particle shape and not the internal variations of scattering density (20-22). In addition, Stuhrmann has developed a mathematical approach for determining complex shapes according to which the scattering data are fit to obtain the coefficients of spherical harmonics which describe a structure compatible with the scattering data (21,22,24-26). This procedure has the advantage of evaluating arbitrary shapes rather than just simple, relatively symmetric ones. Shape analysis however is beset by three major difficulties: accuracy, resolution and uniqueness. Accuracy is of course an experimental problem, but is quite important in the high angle region where the scattering intensity and consequently the statistical accuracy is small. The resolution of scattering curves is always limited because at some scattering angle, the intensity becomes too weak to measure. The lack of data at higher angles limits the details of proposed structures and adjustments of these structures within distances comparable to the

resolution ($\lambda/2\sin\theta_{max}$, where θ_{max} is half the maximum scattering angle) will not result in appreciably better fits to the experimental data. The problem of uniqueness is simply that there is no proof that only one structure will give the experimental scattering. There may be several structures of very different shape which give the appropriate scattering. Because of these three difficulties, shape analysis is usually rather limited. It is of course more useful in establishing that a proposed structure is not the correct one, than that it is. In practice however, additional information, such as biochemical results, component structures, electron microscopy etc. can also contribute to establishing a well-defined, unique, shape.

The examples given here are just a few of many biological studies which have utilized thermal neutron scattering. Many details of these examples have not been included because of lack of space, but the reader is urged to consult the references herein and other papers of a growing literature of biological applications of thermal neutron scattering.

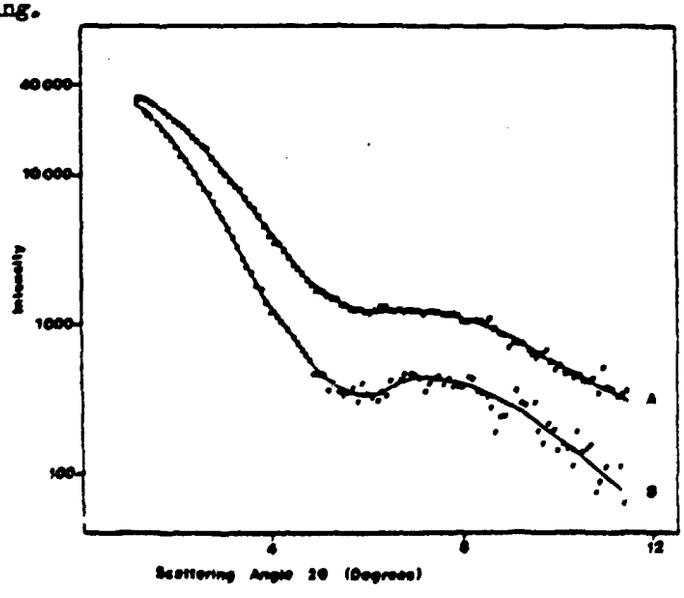

Fig. 17) Neutron scattering profiles from A) Chicken erythrocyte core protein, 12mg/ml, 2M NaCl in D_2O. B) Chromatin subunit particles in D_2O buffer 9mg/ml. (from ref. 33).

References

1) WORCESTER, D.L. (1976). "Biological Applications of Thermal Neutron Scattering: A Bibliography" Harwell report MPD/NES/7. Available from H.M.S.O., U.K.

2) Proceedings of the Brookhaven Symposium in Biology No. 27. June, 1975 (B.P. Schoenborn, editor). Available from: National Technical Information Service, U.S. Dept. of Commerce, 5285 Port Royal Road, Springfield, Virginia 22161, U.S.A.

3) HAYWOOD, B.C.G. and WORCESTER, D.L. (1973). J. Phys. E. 6, 568-571.

4) NUNES, A.C. (1973). Nucl. Inst. and Meth. 108, 189-191.

5) SCHOENBORN, B.P., NUNES, A.C. and NATHANS, R. (1970). Ber. Bunsen-Ges. Phys. Chem. 74, 1202-1205.

6) WORCESTER, D.L. (1976). in "Biological Membranes, Vol. 3" pp.1- 46 (D. Chapman and D.F.H. Wallach, eds) Academic Press, London.

7) WORCESTER, D.L. (1975). in Proceedings of the Brookhaven Symposium in Biology No. 27. pp. III-37 - III-57.

8) WORCESTER, D.L. and FRANKS, N.P. (1976). J. Mol. Biol. 100, 359-378.

9) LUZZATI, V. (1968). In "Biological Membranes". (D. Chapman, ed.), pp.71-123. Academic Press, New York.

10) TARDIEU, A., LUZZATI, V. and Reman, F.C. (1973). J. Mol. Biol. 75, 711-733.

11) LECUYER, H. and DERVICHIAN, D.G. (1969). J. Mol. Biol. 45, 39-50.

12) TORBET, J. (1973). Ph.D. Thesis, University of London.

13) FALKENBERG, P., BUCKLAND, B. and WALSBY , A.E. (1972). Arch. Mikrobiol. 85, 304-9.

14) WALSBY . A.E. and BUCKLAND, B. (1969). Nature 224, 716-717.

15) STOECKENIUS, W. and KUNAU, W.H., J. Cell Biol. 38, 337-57.

16) WALSBY , A.E. (1972). Bacteriol. Rev. 36, 1-32.

17) SADLER, D.M. and WORCESTER, D.L. (1976). in Annual Report of the Institut Laue-Langevin.

18) SCHNEIDER, R., MAYER, A., SCHMATZ, W., KAISER, B. and SCHERM, R. (1969). J. Mol. Biol. 41, 231-235.

19) SCHELTEN, J., SCHLECHT, P., SCHMATZ, W. and MAYER, Q. (1972). J. Biol. Chem. 247, 5436-5441.

20) STUHRMANN, H.B. (1974). J. Appl. Cryst. 7, 173-178.

21) STUHRMANN, H.B. (1975). in Proceedings of the Brookhaven Symposium in Biology No. 27. pp. IV-3 - IV-19.

22) IBEL, K. and STUHRMANN, H.B. (1975). J. Mol. Biol. 93, 255-265.

23) STUHRMANN, H.B., TARDIEU, A., MATEU, L., SARDET, C., LUZZATI, V., AGGERBECK, L. and SCANU, A.M. (1975). Proc. Nat. Acad. Sci. U.S.A. 72, 2270-2273.

24) STUHRMANN, H.B., HAAS, J., IBEL, K., KOCH, M.H.J. and CRICHTON, R.R. (1976). J. Mol. Biol. 100, 399-413.

25) MARGUERIE, G. and STUHRMANN, H.B. (1976). J. Mol. Biol. 102, 143-156.

26) STUHRMANN, H.B. and FUESS, H. (1976). Acta Cryst. A 32, 67-74.

27) STUHRMANN, H.B., HAAS, J., IBEL, K., DeWOLF, B., KOCH, M.H.J., PARFAIT, R. and CRICHTON, R.R. (1976). Proc. Nat. Acad. Sci. U.S.A. 73, 2379-2383.

28) GUINIER, A. and FOURNET, G. (1955). "Small-angle Scattering of X-rays". J. Wiley and Sons, N.Y.

29) PARDON, J.F., WORCESTER, D.L., WOOLEY, J.C., TATCHELL, K., VAN HOLDE, K.E. and RICHARDS, B.M. (1975). Nucleic Acids Research 2, 2163-2176.

30) HJELM, R.P., KNEALE, G.G., SUAU, P., BALDWIN, J.P. and BRADBURY, E.M. (1977). Cell 10, 139-151.

31) YEAGER, M.J. (1975). in Proceedings of the Brookhaven Symposium in Biology No. 27. pp. III-3 - III-36.

32) JACROT, B. (1976). Rep. Prog. Phys. 39, 911-953.

33) RICHARDS, B., COTTER, R., LILLEY, D., PARDON, J., WOOLEY, J. and WORCESTER, D.L. (1976). Current Chromosome Research, pp. 7-16. (K. Jones and P.E. Brandham, eds.)
Elsevier/North Holland.

34) POROD, G. (1948). Acta Phys. Aust. 2, 255-292.

35) MITTELBACH, P. and POROD, G. (1961). Acta Physica Austriaca 14, 185-211.

36) MITTELBACH, P. and POROD, G. (1961). Acta Physica Austriaca 14, 405-439.

DISCUSSION

M. Nève de Mévergnies (Mol)

Are the parasitic fast neutrons present in the incident neutron beam causing any "radiation damage" in the biological sample under study ?

Worcester

The flux of fast neutrons is quite low because of the bismuth filter. The remaining fast neutrons will certainly cause some radiation damage, but it is really a negligible amount. There is also some gamma radiation in the beam. The total radiation damage is much less than occurs in X-ray diffraction. Some lipid samples I have studied have had total exposures of several weeks, and the diffraction patterns were just as strong at the end as at the beginning.

Lekkerkerker (V.U.B., Brussels)

Is it possible to probe with neutron scattering the liquid-like motion of the hydrocarbon chains in the interior of a lipid bilayer ?

Worcester

Yes. Studies of this kind have been made by Dr. H.D. Middendorf of King's College, London. The method, of course is neutron time-of-flight spectroscopy with analysis of the quasi-elastic broadening of the elastic peak. Changes of the fluidity of the hydrocarbon chains with hydration and cholesterol content have been measured but I don't think there have yet been any publication. Detailed interpretation is difficult because rotational and translational diffusion must be seperated.